Biogeochemistry (2008) 88:73–88
DOI 10.1007/s10533-008-9195-6

ORIGINAL PAPER

Effects of wind erosion on the spatial heterogeneity of soil nutrients in two desert grassland communities

Junran Li · Gregory S. Okin · Lorelei Alvarez · Howard Epstein

Received: 13 August 2007 / Accepted: 4 March 2008 / Published online: 19 March 2008

Abstract Wind is known to affect the spatial heterogeneity of soil resources in arid and semiarid systems, but multi-year, quantified observations are largely absent. We studied the effects of wind erosion on the spatial distribution of soil organic carbon (SOC) and other soil nutrients at the Jornada Experimental Range, in southern New Mexico. Enhanced wind erosion was encouraged by grass cover reduction in a *Sporobolus*-mesquite dominated site (SM) and a *Bouteloua*-mesquite dominated site (BM). The scale and magnitude of spatial dependence for the soil analytes were quantified using geostatistical analyses. Results of this study show that soil organic matter related analytes such as SOC, TN, N_{avail}, and $SO_4{}^2$ are among the first to be eroded and redistributed; cations such as Ca^{2+} and Mg^{2+} may not be removed and redistributed significantly; and other ions such as K^+, Na^+ and Cl^- showed no discernible pattern of change. Geostatistics show that wind appeared to increase the scale of spatial autocorrelation, but decrease the scale of spatial dependence of most soil analytes over 2–3 windy seasons. In the wind enhanced plot of the SM site, up to 99% of the spatial dependence of SOC was autocorrelated at the distance of 1.45 m before the initiation of wind erosion, but the spatial dependence dropped significantly to only 60% at a larger autocorrelation distance of 2.76 m after three windy seasons. Similar but less significant changes were observed for SOC in the BM site. Despite the differential effects of wind on the soil analytes, we conclude that the overall results of wind on the grass cover reduction plots are the disappearance of small, strong fertile islands, which may be related to grasses; and the reinforcement of large fertile islands, which are likely related to mesquite shrubs. In addition, the change of the spatial patterns of SOC and other soil nutrients induced by enhanced wind erosion may persist and reinforce soil islands associated with shrubs, thus allowing a positive feedback for further desertification in this arid grassland.

Keywords Spatial heterogeneity · Soil nutrients · Soil carbon · Soil nitrogen · Wind erosion · Geostatistics

J. Li (✉) · L. Alvarez · H. Epstein
Department of Environmental Sciences,
University of Virginia, Clark Hall, 291 McCormick Rd.,
Charlottesville, VA 22904-4123, USA
e-mail: jl2mc@virginia.edu

G. S. Okin
Department of Geography, University of California, 1255
Bunche Hall, Box 951524, Los Angeles, CA 90095, USA

Introduction

Soil resource heterogeneity in arid and semiarid grasslands has been documented in many studies (Virginia and Jarrell 1983; Hook et al. 1991;

Schlesinger et al. 1996; Kieft et al. 1998; Schade and Hobbie 2005). The initiation of such heterogeneity has been explained primarily by overgrazing, which alters the relatively uniform distribution of water, N, and other soil resources (Schlesinger et al. 1990; Franzluebbers et al. 2000; Augustine and Frank 2001). Heterogeneity of soil resources leads to the invasion of these ecosystems by woody shrubs (Schlesinger et al. 1990). During such ecosystem conversion, soil resource distributions change by the movement of resources from plant interspaces to the area beneath plant canopies. This process leads to the development of well-known "islands of fertility," which characterize desert habitats on all continents, but is particularly well described in the American southwest (Crawford and Gosz 1982; Hook et al. 1991; Schlesinger et al. 1996; Schlesinger and Pilmanis 1998; Reynolds et al. 1999).

A great deal of work has examined the role of biotic factors in the reinforcement of islands of fertility in arid and semiarid grasslands; these include the uptake of soil nutrients by vegetation and subsequent deposition of litter (West and Skujins 1977), and higher microbial, invertebrate and vertebrate activities under shrub canopies (Herman et al. 1995). Abiotic factors such as topography, precipitation, fluvial processes, and aeolian activities are known to create spatial heterogeneity in soil properties (Burke 1989; Coppinger et al. 1991; Parsons et al. 1992; Fisk et al. 1998; Okin and Gillette 2001). In arid and semiarid grasslands, the role of water has been the focus of nutrient reduction and redistribution (Parsons et al. 1992; Schlesinger et al. 2000; Augustine and Frank 2001). However, in many desert areas, water-based transport of soil nutrients and particulate matter is limited due to the closed basins and flat terrain (Gillette and Pitchford 2004). Schlesinger et al. (2000) point out that water erosion cannot, by itself, account for the observed depletion and redistribution of soil nutrients in the degraded land in the Chihuahuan Desert. The role of wind in the removal or redistribution of soil resources in natural landscapes has been investigated by only a few studies (Coppinger et al. 1991; Leys and McTainsh 1994; Larney et al. 1998; Okin and Gillette 2001; Li et al. 2007). The study by Li et al. (2007) at the Jornada Experimental Range (JER) in southern New Mexico showed that wind can deplete 25% of soil C and N within three windy seasons. Coppinger et al. (1991) suggest that shrub islands can be enforced by the deposition of windblown materials captured by shrub canopies. Okin and Gillette (2001) demonstrate that aeolian processes must be partially responsible for observed vegetation spatial patterns in the northern Chihuahuan Desert. However, no study to date has monitored the effect of wind on the temporal development of spatial distribution of soil nutrients in arid and semiarid grasslands.

Over the past several decades, studies on the spatial heterogeneity of soil resources associated with plants have changed from mostly descriptive accounts to detailed analyses using spatial statistics (Cain et al. 1999). The latter approach has proven to be valuable for characterizing resource variation across different ecosystems (Schlesinger et al. 1996; Goovaerts 1997; Webster and Oliver 2000). However, most spatial statistical analyses of soil resources are for a single time period only. In this study, we do not focus on the spatial distribution of soil nutrients in different plant communities, which has been extensively investigated by Schlesinger et al. (1996). Instead, we report results from a unique multi-year, vegetation-removal experiment to examine the effects of wind erosion on the spatial distribution of soil nutrients in two Chihuahuan Desert grassland communities with sparse mesquite (*Prosopis glandulosa*). In particular, we investigated (1) temporal changes in soil nutrient variation; and (2) the magnitude of spatial heterogeneity of soil analyte dynamics, and (3) how spatial heterogeneity changes through time in the presence of enhanced wind erosion. In a previous paper, we report aeolian sediment flux and soil nutrient loss from the sites (Li et al. 2007).

Methods

Site description

The study site is located at the USDA-ARS JER, in the northern Chihuahuan Desert, 35 km northeast of Las Cruces, New Mexico. The JER was established in 1912 and now is part of the National Science Foundation's Long Term Ecological Research (LTER) network. Mean annual temperature is 15.6°C, and mean annual precipitation is 247 mm recorded at the JER headquarters, with 52% occurring from July to September (Buffington and Herbel 1965). The erosive winds at JER are highly consistent, with 79% occurring from a southwesterly direction, and dominant wind erosion events happen from early March to May though erosive events can occur anytime throughout the year (Helm and Breed 1999). The mean annual wind speed monitored at a height of 6.1 m is 2.7 m s^{-1}, although during windstorms velocities can exceed 29.8 m s^{-1} (Helm and Breed 1999). Elevation of the JER varies from 1,200 to 1,300 m. The topography of the Jornada Basin consists of gently rolling to nearly level uplands, interspersed with swales and old lake beds (Buffington and Herbel 1965). Soils in the JER are quite complex, but sands and sandy loams are generally widespread (Bulloch and Neher 1977).

Two field sites were located in Pasture 11 of the JER, separated by about 3 km. These two sites represent typical plant communities of the JER. Although both sites are identified as grassland, different grass species dominate each. Site 1 (32°34′09″ N, 106°45′26″ W) is dominated by *Sporobolus* spp. grasses (primarily *S. flexuosus* and *S. contractus*) and mesquites, hereafter referred to as *Sporobolus*-mesquite (SM) site; site 2 (32°33′10″ N, 106°45′48″ W) is dominated by *Bouteloua eriopoda* and mesquites, and is hereafter referred to as *Bouteloua*-mesquite (BM) site. Soils at both sites have sandy texture, normally with coarse sand (0.5–1.0 mm) >95%, and silt and clay <5%. Soils in the SM site had occasional cryptobiotic crusts at the beginning of the experiment, while more frequent cryptobiotic crusts were seen in the BM site at the time the site was selected. Both sites are underlain by a thick petrocalcic horizon >1 m depth. Detailed characteristics of both sites are summarized in Table 1.

Table 1 Environmental characteristics of the study sites

Characteristics	*Sporobolus*-mesquite site (SM site)[a]		*Bouteloua*-mesquite site (BM site)[a]	
	T100	Control	T100	Control
Wind erosion (g m^{-1} day^{-1}, means ±1 SD)[b]	454 ± 179[c]	18 ± 8[c]	790 ± 561[d]	21 ± 5[d]
Plant cover (%)				
Total cover	25	19	22	27
Grass	9	12	13	12
Prosopis	11	3	6	7
Gutierrezia	4	<1	<1	<1
Forb	1	2	3	7
Shrub size (m, means ±1 SD)	1.40 ± 0.69	1.19 ± 0.36	2.15 ± 0.85	1.15 ± 0.47
Surface soil				
Sand (%)	98	97	95	94
Silt and clay (%)	2	3	5	6
Texture	Sand		Sand	
Caliche exposure	No		No	
Biological crust	Rare		Frequently seen	
Geomorphology				
Slope (%)	<1		<1	
Parent material	Wind-reworked fluvial sands		Wind-reworked fluvial sands	
Mesquite dunes	Small-no		No	

Properties were observed before the manipulation of grass cover reduction except for wind erosion, which was monitored in 2004–2006 after grass cover reduction

[a] Description of the site and plot set up can be found in Fig. 1

[b] Wind erosion was represented by sediment flux measured according the method described in *Methods: Experimental design and sampling method*

[c] Measured in Li et al. (2007)

[d] Measured in this study

Experimental design and sampling method

The field experiment was established in March 2004 for the SM site and July 2004 for the BM site. Experimental layout and sampling method for both sites are exactly the same (Fig. 1). In each site, two 25 × 50 m plots, including one wind erosion enhanced plot and one control plot, are aligned parallel to prevailing winds. In the wind erosion enhanced plots (T100), all grasses, perennial semi-shrubs such as *Gutierrezia sarothrae*, and perennial forbs were removed (hereafter referred to as "grass cover reduction" only). No vegetation cover was removed from the control plot. Shrub cover was low in both sites at the beginning of the experiment, and shrubs were not removed.

Within each plot, two 5 × 10 m subplots (named U1 and U2) were set up to collect surface soil samples and to install windblown sediment samplers. Soil sampling was conducted in the U1 subplots located in the center of the 25 × 50 m plots (Fig. 1). In each sampling area, 50 soil samples of 2.5 cm diameter were taken from the top 5 cm before the vegetation removal in March 2004 and July 2004 for the SM and BM sites, respectively. Subsequent soil samples were taken in July 2004, 2005 and 2006 for the SM site, and July 2005 and 2006 for the BM site. Soils had a volumetric moisture content of <3% at the time of collection. Soil samples were randomly distributed with their locations chosen without regard to plant locations, and a different set of sampling coordinates were adopted for each sampling time. Sample locations were determined beforehand using a random number table and the locations of each soil sample were precisely identified for geostatistical analysis.

Six clusters of Big Spring Number Eight (BSNE) sediment samplers (Fryrear 1986) were installed in both 5 × 10 m subplots in each plot (Fig. 1). A cluster comprised an upright post with four samplers positioned approximately 0.1, 0.3, 0.6, and 1.2 m above the soil surface. Windblown sediment samples were collected twice per year in early March (sampling period from previous July to March) and middle July (sampling period from March to July) from 2004 to 2006. Wind erosion rates, represented by sediment flux, were calculated according to Gillette et al. (1997) and presented formally in Li et al. (2007).

Plant cover and community composition on each plot were monitored by three 50-m line-intercept transects before and after the grass cover reduction. Reduced cover on the plots was maintained during the entire experimental period. In addition, the locations of plants in the soil sampling subplots (U1, Fig. 1) were recorded using a Trimble 3600 Total Station System; height and basal area of each plant were also measured.

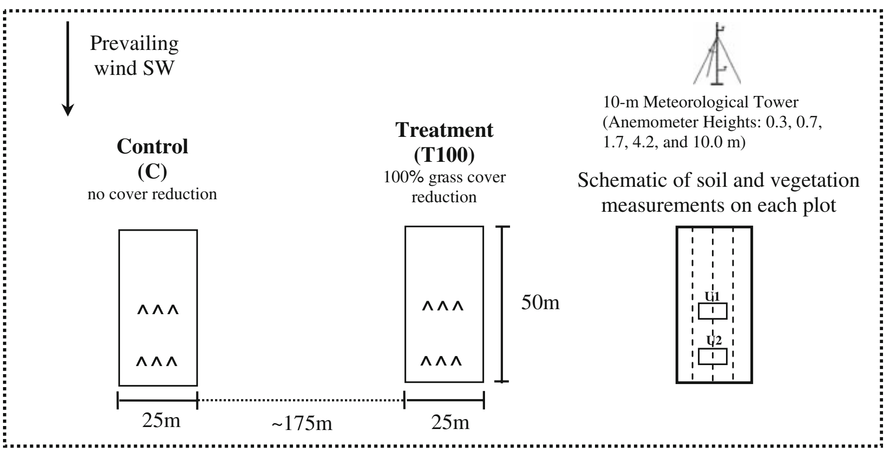

Fig. 1 Experimental layout in the field. The right-most figure shows more detailed layout of sampling locations in each treatment. Soil sampling was conducted in the U1 subplots, BSNEs (represented by "^") were installed in both U1 and U2 subplots. Climatic data were monitored by a 10-m meteorological tower in the further upwind of the plot area. Three 50-m line-intercept transects were set up for plant community monitoring (denoted by dashed line). The field site was fence-protected

Laboratory analysis

In the laboratory, each soil sample was air-dried and sieved through a 2-mm screen to remove roots, debris and gravel. Each windblown sediment sample collected from the BSNEs was weighed to 0.001 g to yield sediment flux. Soil organic carbon (SOC) and total nitrogen (TN) were analyzed on a Shimadzu TOC-V_{CSN} total organic carbon analyzer with a SSM-5000 solid sample accessory and a TNM-1 total nitrogen measuring unit. In this system, SOC was calculated as the difference between total carbon (TC) and total inorganic carbon (TIC). For the analysis of water-extractable anions in the soils, approximately 6 g of subsample was shaken on an end-over-end shaker with 30 ml of deionized water for 30 min, and centrifuged at 4,500 rpm for 10 min. Extracts were analyzed on a Dionex ICS-2000 ion chromatograph with an Ion Pac AS 18 anion exchange column and a 4 μm inline filter for the concentration of Cl^-, NO_2^-, NO_3^-, SO_4^{2-}, and PO_4^{3-}.

Exchangeable cations, such as Na^+, K^+, Mg^{2+}, and Ca^{2+} were analyzed by $BaCl_2$ extraction method according to Hendershot and Duquette (1986). In this method, a 3 g subsample of each soil was added to 30 ml of 0.1 mol l^{-1} $BaCl_2$ solution, shaken slowly on an end-over-end shaker for 2 h, and centrifuged at 4,500 rpm for 10 min. Extracts were analyzed on a Dionex ICS-2000 ion chromatograph with an Ion Pac CS 12A cation exchange column and a 4 μm inline filter. The studies by Horn et al. (1982) and Gillman et al. (1983) indicate that the $BaCl_2$ extraction method gives comparable results to procedures using NH_4CH_3COO and KCl extractions for K^+ and non-K^+ cations, respectively.

For this study, NH_4^+ was also extracted with the 0.1 mol l^{-1} $BaCl_2$ solution. We compared the efficiency of $BaCl_2$ extraction of NH_4^+ to the traditional KCl extraction method. NH_4^+ measured from the 2 mol l^{-1} KCl extract was highly correlated ($r = 0.96$) to NH_4^+ in the 0.1 mol l^{-1} $BaCl_2$ extract. The $BaCl_2$ extraction yielded values that were 2.21 ± 0.56 times greater than those from the KCl extraction. The strong correlation suggests that the $BaCl_2$ extraction should be a dependable index of NH_4^+ availability. Additionally, the $BaCl_2$ extraction method allowed us to analyze all cations simultaneously on the ion chromatograph since the chromatogram peak of Ba^{2+} appears well behind the cations of interest. All soil data were reported as milligrams analyte per kilogram of soil unless otherwise specified. We reported the sum of NO_2^-, NO_3^- and NH_4^+ as the index of total available N (N_{avail}).

Statistical analyses

Modified paired *t*-tests using PASSAGE software (http://www.passagesoftware.net/) were conducted to compare the mean value for the wind erosion enhanced and control plots in both study sites in different years. This modified *t*-test corrects the degrees of freedom considering the amount of autocorrelation in the data (Wang et al. 2007). To describe the overall variation of analytes in soil samples, the coefficient of variation (CV) was computed. Geostatistical analysis was used to infer the size and strength of soil resource patchiness in the plots, as well as how these change through time. We adjusted the soil data set to approximately a normal distribution using a natural logarithmic transformation prior to analysis (Webster and Oliver 2000). A semivariogram was constructed for each analyte for each sampling period and subplot. We compared isotropic and corresponding anisotropic semivariograms at 0°, 45°, 90°, and 135°, and did not find any significant directional patterns. Therefore, isotropic semivariograms were used. Detailed description of patterns and ecological implications of semivariograms can be found in Schlesinger et al. (1996) and Augustine and Frank (2001).

Experimental semivariograms were fit using the jackknife method, presented by Shafer and Varljen (1990) and discussed by Huisman et al. (2003), in a code written in the Interactive Data Language (IDL). We used the lag interval of 0.2 m and lag distance of 3.0 m to calculate the experimental semivariograms for the pretreatment and control plots. Slightly larger lag intervals and lag distances were used to better describe the potential change of soil spatial distributions with the continuation of wind erosion. All semivariograms were fit to a spherical model using a non-linear least squares fit employing the Levenberg-Marquardt algorithm, which combines the steepest descent and inverse-Hessian function fitting methods

(Press et al. 1992). The formula used for this model is:

$$\gamma(h) = C_0 + C[1.5(h/A_0) - 0.5(h/A_0)^3] \; if \; h \le A_0 \quad (1)$$

and

$$\gamma(h) = C_0 + C \quad if \quad h > A_0 \quad (2)$$

where h is the lag interval, A_0 is the range, C_0 is the nugget variance, and C is the structural variance. The uncertainties (95% confidence limits) were determined using the variance-covariance method of Pardo-Iguzquiza and Dowd (2001). The nugget (C_0) denotes the y-intercept of the semivariogram and incorporates random or non-spatial errors, as well as errors associated with spatial variability at finer scales than those measured (Schlesinger et al. 1996). A high nugget variance indicates that most variance occurs over short distances or is due to measurement/locational error (Schlesinger et al. 1996). The magnitude of spatial dependence was calculated using the index of $C/(C_0 + C)$. As this index approaches 1.0, a greater proportion of the total sample variance is spatially structured (Jackson and Caldwell 1993). The distance of the spatial dependence is indicated by the model range A_0. Samples separated by distances smaller than the range are correlated as a result of their proximity to one another, whereas samples separated by greater distances are effectively independent. For our purposes here, variogram parameters are considered significantly different if they do not have overlapping 95% confidence intervals.

In addition to the semivariance analysis, we further produced kriged maps of SOC using calculated semivariograms (GS$^+$ version 7.0, Gamma Design Software, Plainwell, Michigan). Maps were produced following an ordinary block kriging approach with a block size of 2 × 2 m^2. After kriging, we evaluated the interpolation result quality by leave-one-out (LOO) cross-validation. The cross-validation technique consisted of comparing actual values at each point (q_{true}) with kriged value using the entire dataset minus each point in turn (q_{pred}). The results of cross-validation were given by standardized errors, calculated according to the following:

$$\delta_{\text{std}} = \frac{q_{\text{pred}} - q_{\text{true}}}{\sigma} \quad (3)$$

where δ_{std} is the standardized error, σ is the standard deviation of the errors. If the mean of this standardized error ($\overline{\delta_{\text{std}}}$) is zero and the standard deviation is approximately 1, then the model and the method employed provide an acceptable description of the data (Isaaks and Srivastava 1989; Stelzenmüller et al. 2006).

Results

Plot-scale comparisons of analytes

The mean values of soil analytes were frequently higher in the T100 plots than in the control plots at both study sites at the beginning of the experiment (Table 2, $p < 0.01$, paired t-test). With the continuation of the wind erosion, mean values for a large number of soil analytes in the T100 plots declined significantly compared to those of the control plots, largely due to the depletion of soil analytes in the T100 plots and the slight accumulation in the control plots. In particular, soil TN in the T100 plots in both the SM and BM sites, and SOC in the T100 plot in the SM site decreased consistently relative to the control plots during the experimental period. Despite significant variation between different sampling times, soluble ions such as SO_4^{2-}, Cl^-, and Na^+ did not show consistent changes in the T100 plots relative to the control plots.

Our focus in this study was spatial variation in soil analytes. In both sites, enhanced wind erosion altered the total amount of variation in soil analytes over 2–3 windy seasons (Table 3). Initially, the overall variation of soil analytes in the SM site (both the T100 and the control plots) was higher than those of the BM site. In addition, CVs were always highest for soluble ions such as Cl^- and SO_4^{2-} and lowest CVs were generally found for ions such as PO_4^{3-}, Mg^{2+}, Ca^{2+}, and K^+.

In the SM site, the ratios of CVs between the T100 and the control plots for SOC and TN declined steadily from ~2.0 in March 2004 to ~1.0 in July 2006. In the mean time, CVs in the T100 relative to the control plots for N_{avail}, PO_4^{3-}, K^+, and Cl^- declined substantially in July 2006 compared to pre-grass cover reduction (March 2004). In contrast, CVs in the T100 relative to the control plots in the BM site decreased insignificantly with the continuation of wind erosion (July 2004–July 2006), especially for N_{avail}, K^+, PO_4^{3-}, and Ca^{2+}.

Table 2 The mean concentration of analytes measured in the grass cover reduction plots (T100) and the control plots (C) during the experimental period ($n = 50$)

Analyte ($mg\ kg^{-1}$)	March 2004		July 2004		July 2005		July 2006	
	T100	C	T100	C	T100	C	T100	C
(a) *Sporobolus*-mesquite site								
SOC[a]	3.1	2.5	2.6	2.7	2.4*	3.0	2.2*	3.2
TN	335.2*	285.7	287.9	287.6	266.4*	318.6	242.2*	344.6
N_{avail}	41.8*	16.2	24.7*	36.1	17.8	19.9	10.6*	22.9
PO_4^{3-}	8.1*	6.5	6.7	6.6	7.9*	6.3	7.2	7.0
K^+	178.8	165.1	162.2*	133	133.9*	120.1	129.6*	115.3
Mg^{2+}	92.2*	71.4	99.5*	68.8	82.3*	55.7	82.8*	57.3
Ca^{2+}	534.7	512.5	571.4	551.2	474.2	433.9	464.0	453.9
SO_4^{2-}	6.9*	9.3	5.4	5.0	4.3	4.2	0.7*	2.4
Cl	1.4	1.5	1.3*	5.9	1.2*	1.9	0.2*	0.6
Na^+	6.4	7.2	8.0*	10.7	7.2	8.2	5.5*	6.9
(b) *Bouteloua*-mesquite site								
SOC[a]			3.4	3.2	3.0	3.3	2.9	3.2
TN			408.5*	292.3	349.5	386.8	323.3*	391.1
N_{avail}			36.4*	14.1	38.3*	10.0	9.6*	13.5
PO_4^{3-}			3.4*	4.9	4.4*	5.1	4.2*	5.2
K^+			131.4*	169.3	119.3*	142.2	132.3	133.2
Mg^{2+}			63.3*	71.6	52.5*	73.6	56.5*	73.1
Ca^{2+}			1175.8	1084.7	1095*	941.6	1081.8*	954.8
SO_4^{2-}			2.7*	4.8	1.4*	2.0	0.9	1.0
Cl^-			0.5*	1.0	0.6	0.5	0.2*	0.3
Na^+			9.6*	4.2	4.7*	11.2	4.9*	5.7

Asterisks indicate significant differences between wind erosion enhanced (T100) versus control plots at individual sampling times (paired *t*-test at $p < 0.01$ for significance).

[a] Units of $g\ kg^{-1}$

Geostatistical analyses

For the semivariograms of each soil analyte, we reported the estimates of the spatial dependence index $C/(C_0 + C)$, range A_0, and the standard deviation of these parameters pre and post-grass cover reduction. In addition, the mean standardized errors $\overline{\delta_{std}}$ (MSR) of the cross-validation are also presented (Table 4 and Appendix 1 for all sampling periods).

Spatial distribution of soil analytes

The spherical model generally provides a good fit to the semivariograms. Standard deviation of the standardized errors, $\sigma(\delta_{std})$, for analytes with nonrandom distribution ranged from 0.99 to 1.08. Z-score (i.e. $\overline{\delta_{std}}/\sigma(\delta_{std})$) for all fits are less than 2, indicating that the spherical model is a sufficient model for the data.

The Sporobolus-mesquite site (SM) At the beginning of the experiment (March 2004), all the soil analytes examined, except for PO_4^{3-}, were autocorrelated over mean distances of 0.96–1.69 m. Soil PO_4^{3-} was autocorrelated at a mean distance of 2.43 m, which is significantly greater than most of the other analytes (Table 4a). In contrast to the T100 plot, soil analytes in the control plot were autocorrelated over smaller distances of 0.51–1.61 m, but they were not significantly different from those of the T100 plot except in the case of Mg^{2+} and PO_4^{3-} (Table 4a). Geostatistics further show the degree of spatial dependence at distances >0.2 m to be 71–

Table 3 Changes of coefficient of variation (100% (SD/Mean)) for the overall concentration of soil analytes in the grass cover reduction plots (T100) and the control plots (C) during the experimental period ($n = 50$)

Analyte	March 2004			July 2004			July 2005			July 2006		
	T100	C	Ratio	T100	C	Ratio	T100	C	Ratio	T100	C	Ratio
(a) *Sporobolus*-mesquite site												
SOC	57	31	1.84	46	34	1.35	44	42	1.05	38	35	1.09
TN	41	21	1.95	28	21	1.33	27	27	1.00	21	26	0.81
N_{avail}	59	84	0.70	104	74	1.41	87	97	0.90	38	69	0.55
PO_4^{3-}	29	28	1.04	21	31	0.68	25	36	0.69	19	23	0.83
K^+	50	57	0.88	28	43	0.65	30	23	1.30	18	25	0.72
Mg^{2+}	22	22	1.00	19	28	0.68	20	27	0.74	23	21	1.10
Ca^{2+}	18	20	0.90	18	37	0.49	22	20	1.10	22	20	1.10
SO_4^{2-}	112	252	0.44	177	108	1.64	159	98	1.62	234	229	1.02
Cl^-	197	199	0.99	171	101	1.69	150	88	1.70	86	173	0.50
Na^+	273	200	1.37	345	232	1.49	13	15	0.87	28	14	2.00
(b) *Bouteloua*-mesquite site												
SOC				36	25	1.44	32	35	0.91	29	26	1.12
TN				21	26	0.81	26	21	1.24	22	26	0.85
N_{avail}				72	56	1.29	77	69	1.12	54	44	1.23
PO_4^{3-}				26	19	1.37	25	26	0.96	26	20	1.30
K^+				25	29	0.86	15	37	0.41	16	20	0.80
Mg^{2+}				26	16	1.63	22	28	0.79	16	29	0.55
Ca^{2+}				22	18	1.22	17	15	1.13	17	16	1.06
SO_4^{2-}				65	48	1.35	120	91	1.32	34	73	0.47
Cl^-				63	103	0.61	207	85	2.44	70	77	0.91
Na^+				11	42	0.26	21	12	1.75	15	30	0.50

100% for March 2004. Significant differences in the spatial dependence between T100 and control plots were only found for PO_4^{3-}.

After three windy seasons, the range of autocorrelation for TOC, TN, N_{avail}, and Mg^{2+} in the T100 plot increased significantly relative to that of the control plot (Table 4a, Fig. 2a). In the meantime, the magnitude of spatial dependence in the T100 plot generally declined, with significant changes compared to the control plot for SOC and Mg^{2+}. Other soil nutrients, such as Ca^{2+}, SO_4^{2-}, Cl^-, and Na^+, actually changed from patterned to random, with most of the spatial variation found at distances <0.2 m (Table 4a, Fig. 3a).

The Bouteloua-mesquite site (BM) Before grass cover reduction (July 2004), soil analytes in the BM site were more frequently randomly distributed (such as K^+, Cl^- and Na^+) than those of the SM site. For those soil variables with patterned distribution, the scale of autocorrelation ranged over mean distances of 0.47 m (PO_4^{3-}) to 3.24 m (SOC), and >64% of the variance was spatially dependent.

By July 2006, the scale of the autocorrelation of SOC increased slightly in the T100 plot and the significant difference of SOC between T100 and the control plot was maintained. The magnitude of spatial dependence in soil analytes changed little except for SOC, which dropped from 97% to 67% after two windy seasons, a significant decrease compared to that of the control plot (Table 4b, Fig. 3b). Overall, patterned distributions with high spatial dependence were more frequently found in the SM site than in the BM site. In both study sites, soil nutrients with random distributions were primarily Na^+ and Cl^-, and also K^+, SO_4^{2-}, and Ca^{2+}.

Kriging analysis and cross-validation

The small mean standardized error derived from cross-validation indicates that the model and the

Table 4 Summary of the semivariogram model parameters in both study sites before and after grass cover reduction

Analyte	A_0 (m)		$C/(C_0 + C)$		MSR	
	T100	Control	T100	Control	T100	Control
(a) *Sporobolus*-mesquite site						
March 2004 (pre-grass cover reduction)						
SOC	1.45 (0.23)	1.48 (0.32)	0.99 (0.14)	0.71 (0.19)	0.13	0.10
TN	1.39 (0.24)	1.22 (0.25)	0.99 (0.15)	0.90 (0.13)	0.16	0.19
N_{avail}	1.58 (0.23)	1.59 (0.29)	0.87 (0.09)	0.77 (0.14)	0.05	−0.08
PO_4^{3-}	2.43 (0.50)*	1.61 (0.22)	0.71 (0.12)*	0.99 (0.12)	−0.03	0.01
K^+	0.96 (0.18)	0.78 (0.14)	0.99 (0.15)	0.98 (0.13)	0.01	0.04
Mg^{2+}	1.28 (0.31)*	0.51 (0.25)	0.74 (0.16)	0.99 (0.27)	0.06	0.11
Ca^{2+}	1.69 (0.26)	1.22 (0.25)	0.75 (0.13)	0.92 (0.16)	0.07	0.16
SO_4^{2-}	1.16 (0.15)	1.03 (0.20)	0.96 (0.15)	0.99 (0.08)	−0.06	0.05
Cl^-	1.35 (0.17)	1.32 (0.23)	0.97 (0.11)	0.99 (0.07)	0.04	0.10
Na^+	0.96 (0.19)	0.87 (0.19)	0.99 (0.90)	0.85 (0.17)	0.11	0.06
Jul. 06 (post-grass cover reduction)						
SOC	2.76 (0.50)*	1.97 (0.23)	0.60 (0.11)*	0.89 (0.09)	−0.01	0.02
TN	3.96 (0.72)*	1.70 (0.31)	0.66 (0.14)	0.69 (0.25)	0.09	0.06
N_{avail}	3.93 (0.44)*	1.50 (0.55)	0.75 (0.16)	0.63 (0.12)	−0.07	−0.07
PO_4^{3-}	2.31 (0.41)	2.10 (0.42)	0.66 (0.16)	0.63 (0.15)	0.01	0.03
K^+	0.89 (0.24)	0.54 (0.60)	0.77 (0.19)	0.99 (0.23)	0.03	0.09
Mg^{2+}	2.75 (0.31)*	1.34 (0.22)	0.76 (0.11)*	0.99 (0.13)	−0.03	0.00
Ca^{2+}	<0.2	2.05 (0.24)	–	0.90 (0.10)	–	0.07
SO_4^{2-}	<0.2	1.25 (0.27)	–	0.85 (0.20)	–	−0.11
Cl^-	<0.2	1.38 (0.31)	–	0.88 (0.16)	–	0.09
Na^+	<0.2	<0.2	–	–	–	–
(b) *Bouteloua*-mesquite site						
July 2004 (pre-grass cover reduction)						
SOC	3.24 (0.34)*	1.06 (0.29)	0.97 (0.08)	0.77 (0.21)	−0.02	0.05
TN	0.99 (0.32)	1.12 (0.23)	0.64 (0.22)	0.78 (0.17)	0.04	0.03
N_{avail}	1.48 (0.28)*	1.00 (0.19)	0.78 (0.16)	0.99 (0.13)	−0.20	0.06
PO_4^{3-}	0.47 (0.55)	0.88 (0.21)	0.67 (0.44)	0.89 (0.16)	0.16	0.07
K^+	<0.2	1.63 (0.22)	–	0.98 (0.06)	–	0.07
Mg^{2+}	1.00 (0.22)	0.98 (0.26)	0.99 (0.13)	0.86 (0.17)	0.08	0.04
Ca^{2+}	0.83 (0.13)*	2.54 (0.30)	0.99 (0.12)	0.80 (0.11)	0.06	0.04
SO_4^{2-}	2.32 (0.32)*	1.01 (0.36)	0.74 (0.12)	0.67 (0.21)	0.00	0.08
Cl^-	<0.2	0.90 (0.21)	–	1.00 (0.17)	–	0.06
Na^+	<0.2	–	–	–	–	–
July 2006 (post-grass cover reduction)						
SOC	3.51 (0.40)*	1.25 (0.25)	0.67 (0.08)*	0.96 (0.11)	0.02	0.03
TN	1.55 (0.38)	1.00 (0.46)	0.67 (0.16)	0.57 (0.20)	0.06	0.04
N_{avail}	2.20 (0.25)	<0.2	0.88 (0.11)	–	−0.07	–
PO_4^{3-}	1.00 (0.41)	>3.0	0.68 (0.22)	–	0.03	–
K^+	<0.2	1.59 (0.46)	–	0.61 (0.17)	–	0.05
Mg^{2+}	<0.2	1.12 (0.40)	–	0.72 (0.24)	–	0.09
Ca^{2+}	3.26 (0.61)	2.45 (0.48)	0.59 (0.13)	0.62 (0.15)	0.07	0.07

Table 4 continued

Analyte	A_0 (m)		$C/(C_0 + C)$		MSR	
	T100	Control	T100	Control	T100	Control
SO_4^{2-}	0.92 (0.31)	>3.0	0.99 (0.25)	–	−0.11	–
Cl^-	2.16 (0.68)	<0.2	0.59 (0.18)	–	0.14	–
Na^+	<0.2	<0.2	–	–	–	–

Results for $C/(C_0 + C)$ and A_0 are means and 1 standard deviation (in the parentheses). MSR is the mean standardized error derived from the cross-validation. "–" indicates random distribution and no data available. "*" indicates significant differences between wind erosion enhanced versus control plots at a 95% confidence level

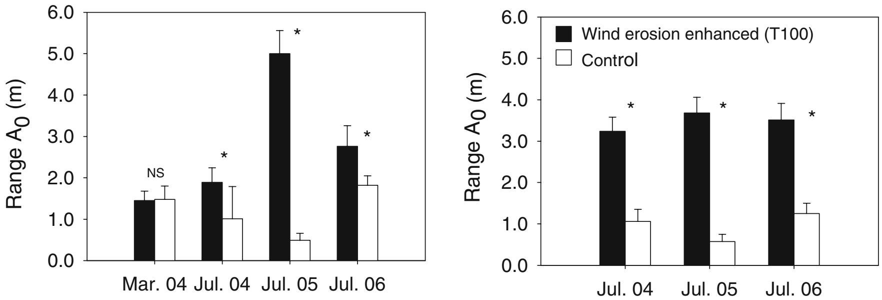

(a) *Sporobolus*-mesquite site **(b)** *Bouteloua*-mesquite site

Fig. 2 The scale of the spatial autocorrelation (A_0) of soil organic carbon (SOC) affected by enhanced wind erosion. Range of the T100 plot in July 2005 for the *sporobolus*-mesquite site was actually greater than 5 m and it was take as 5 m to facilitate graphing. Error bars are 1 standard deviation. Asterisks indicate significant differences between wind erosion enhanced versus control plots at a 95% confidence level, and NS indicates no significant difference

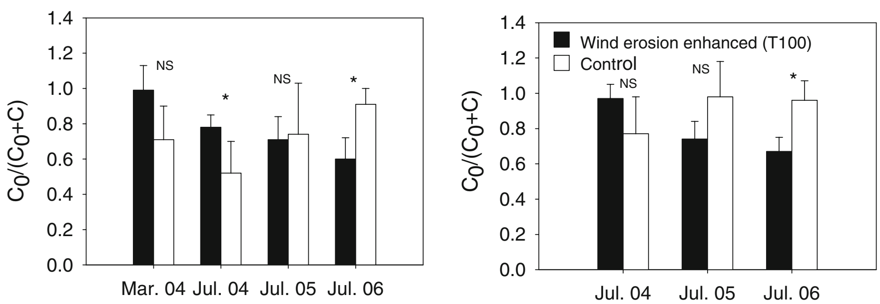

(a) *Sporobolus*-mesquite site **(b)** *Bouteloua*-mesquite site

Fig. 3 The magnitude of spatial dependence ($C_0/(C_0 + C)$) of soil organic carbon (SOC) affected by enhanced wind erosion. Error bars are 1 standard deviation but the upper limit of the index $C_0/(C_0 + C)$ is 1.0. Asterisks indicate significant differences between wind erosion enhanced versus control plots at a 95% confidence level, and NS indicates no significant difference

selected parameters used in the kriging were adequate (Table 4a, b). To illustrate the change in spatial distribution of soil analytes under enhanced wind erosion, the maps of SOC are presented (Fig. 4). Clearly, the maps show high variation in the SM site, which was also observed in the results obtained by the conventional statistical methods (Table 2). The maps also reveal that there were stronger patches of SOC in the SM site than in the BM site, corresponding to the more frequent distribution of mesquite shrubs in the former than in the latter (Table 1). The influences of grass cover reduction and enhanced

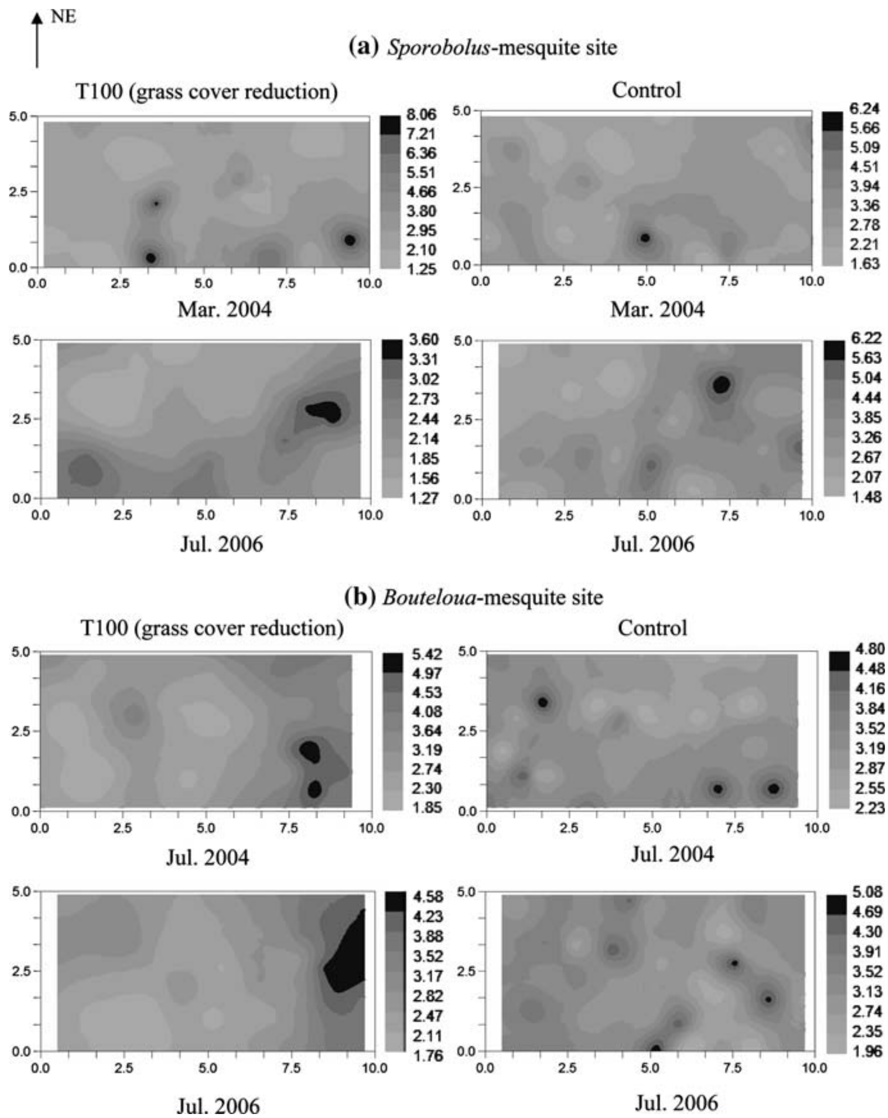

Fig. 4 Spatial distribution of soil organic carbon (SOC, g kg^{-1}) predicted by kriging analysis in the 5 × 10 m soil sampling subplots in the grass cover reduction (T100) and the control plots (C)

wind erosion on the spatial distribution of SOC are also visible. In July 2006, essentially no strong patches were observed, and larger-sized, relatively weak patches were formed. Similar observations were made in the BM site. By the end of the field experiment in July 2006, no strong patches were seen.

Discussion

Although a few studies have examined the spatial characteristics of soil properties in arid and semiarid grasslands (Ludwig et al. 1975; Jackson and Caldwell 1993; Schlesinger et al. 1996; Larney et al. 1998; Augustine and Frank 2001), none of them have conducted a multi-year investigation on the role of wind. Results from this study and a previous study by Li et al. (2007) show that wind erosion depleted SOC and a variety of soil nutrients, and changed their spatial distribution patterns significantly over 2–3 windy seasons. Calculations of coefficient of variation (CV) indicate that soil analytes in the plots with higher cover of mesquite shrubs (SM site) are generally more variable than those of the plots with a higher cover of black grama grasses (BM site) (Table 2). Such patterns were consistent with the observations of Schlesinger et al. (1990, 1996) in the JER and in the Great Basin shrublands and grasslands.

After the elimination of grass cover, the overall variation of most of the soil variables in the wind enhanced plots declined in both study sites, indicating that wind has homogenized the distribution of soil variables without the presence of grasses (Table 2).

Geostatistics augment the ability of conventional statistics to compare the size and strength of soil nutrient patches before and after the introduction of enhanced wind erosion. Initially, the spherical model provides a good fit to the semivariogram for all the soil analytes in the site dominated by *Sporobolus* spp. and mesquites (SM site). However, with the presence of more *Bouteloua* grasses (BM site), soil Na^+, Cl^-, and K^+ were spatially independent with most of the variation occurring at distances <0.2 m, which is unlikely to be related to nutrient cycling by shrubs. High variation of Na^+ and Cl^- at a small spatial scale <0.2 m has also been reported by Schlesinger et al. (1996) in a *Bouteloua eriopoda* dominated grassland at the JER. Before the reduction of grass cover, geostatistics further show that for those soil analytes with patterned distribution, most of the variation occurs over spatially autocorrelated distances from ~1.0 m to 3.0 m (except for SOC in the T100 plot of the BM site in July 2004) (Table 4), close to the mean size of mesquite shrubs measured at the sites (Table 1). In a shrubland ecosystem dominated by *Larrea tridentata* at the JER, Schlesinger et al. (1996) found that soil N_{avail} is autocorrelated over distances extending 1.0–3.0 m. Jackson and Caldwell (1993) report that soil N, P, and K were spatially dependent within 1.0 m in shrublands of the Great Basin Desert of Utah.

Geostatistics demonstrate that enhanced wind erosion appears to increase the spatial autocorrelation distance and decrease the spatial dependence in both study sites (Table 4, Figs. 2, 3). Despite its importance in biogeochemical transformations in soils of arid and semiarid grasslands (Baldock and Nelson 2000), the dynamics of SOC has not been well quantified in previous studies, especially in the presence of significant wind erosion. In the T100 plot of the SM site, in addition to a significant decrease in the mean value and CV (Tables 2, 3), the range of spatial autocorrelation of SOC nearly doubled (1.45 m to 2.76 m) (Fig. 2), and the distribution of SOC dropped from highly (99%) to moderately spatially dependent (60%) by the third windy season (July 2006). Similar but less significant changes in the spatial patterns of SOC also occurred in the T100 plot of the BM site, suggesting that SOC is one of the soil variables that is most responsive to enhanced wind erosion. Kriging maps of SOC visibly show that the change in the spatial distribution patterns of SOC may be associated with the dynamics of fertile islands formed under bunchgrasses or shrubs (Figs. 4, 5). We speculate that the decline of the spatial dependence as well as the total variation may be related to the overall homogenization of soils in the inter-shrub spaces that were previously covered by grasses. Some of the soil nutrients associated with soil particles or plant litter may be permanently lost from the local ecosystem through dust emission, explaining the depletion of mean SOC and other nutrients (Table 2). Most of the soil variables may be redistributed under or captured by mesquite shrubs, resulting in the growth of fertile islands.

Less significant changes in the spatial distribution of soil variables in the BM site compared to the SM site is likely not due to wind erosion intensity differences between sites, since sediment flux in the former was generally greater than that of the latter (Table 1). Instead, we suggest that such differences may stem from soil spatial distribution patterns associated with the original plant cover. In the BM site, the distribution of *Bouteloua* was widely spread or discontinuous with small gaps, resulting in low soil spatial variation and small microtopographic variation at the site (Fig. 5). On the other hand, the dominant grass in the SM site is *Sporobolus flexuosus*, which is a perennial bunchgrass with relative large gaps between the individuals (Fig. 5). These long-lived, drought-resistant grasses are able to create small mounts and micro-fertile islands by increasing water infiltration from stem flow along leaves and tillers, and trapping nutrient enriched windblown particles with leaves and tillers (Tongway and Hindley 2000). With the elimination of these grasses, mounds may be subject to enhanced wind erosion and intense solar radiation, and organic debris accumulated in the depressions may be depleted quickly by enhanced wind erosion (Whitford 2002). These factors may have contributed directly to the filling of depressions and leveling of mounds, and the homogenization of the soil in the grass cover reduction plots (Nash et al. 2004). However, some of this debris along with airborne particles may also be trapped under mesquites on the plots or nearby, resulting in the reinforcement of large fertile islands.

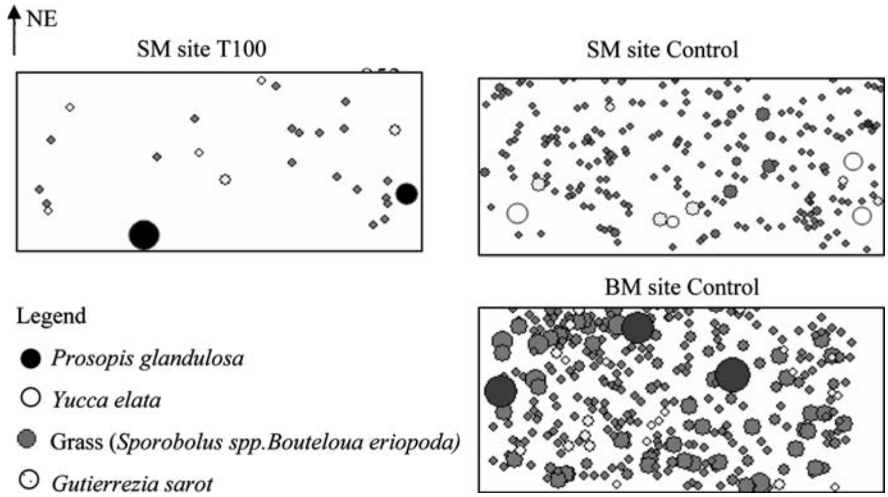

Fig. 5 Distribution of plants in the 5 × 10 m soil sampling subplots in the grass cover reduction (T100) and the control plots (C). No plants were presented in the T100 plot of the BM site after grass cover reduction. The size of the symbols represents the approximate size of the plants

Results of this study also show considerable variation in soil analytes in the control plots (Tables 2–4), implying that other environmental factors might have interacted with wind erosion to cause changes in nutrient concentrations and their spatial characteristics. Parsons et al. (1992) suggest that differential rainsplash, as a result of the dissipation of raindrop energy in the shrub canopy, also results in the directional transport of soil materials toward shrub islands. Similar to the grass cover reduction plots, mounds and depressions associated with the distribution of grasses can affect water infiltration, soil water storage, and erosion by water and wind in the control plot (Nash et al. 2004; Whitford 2002). During the experimental period, high variations were mostly found among Na^+, Cl^-, SO_4^{2}, and K^+, while low variations occurred generally in PO_4^{3-}, Mg^{2+}, and Ca^{2+}. The former group of ions is characterized as soluble and mobile in the environment (Hartley et al. 2007), indicating that leaching and water runoff may be important in determining the distribution of such ions in desert grasslands. For example, Troeh and Thompson (2005) suggest that leaching of anions such as SO_4^{2-} and Cl^- may be favored in desert soils with high pH and low anion-exchange capacity (Lajtha and Schlesinger 1988). The latter group is generally retained by soil and mineral particles (Cross and Schlesinger 2001; Scholes and Walker 2004), resisting the lifting potential by wind and redistribution by runoff. The yearly variations in the mean value of soil analytes in the control plots, thus may be related to interannual variability in precipitation during the experimental period (Li et al. 2007).

Conclusions

While much previous work on the spatial distribution of soil nutrients in desert grasslands has focused on biotic factors and the role of water (West and Skujins 1977; Herman et al. 1995; Parsons et al. 1992; Schlesinger et al. 2000), the effect of wind has largely been overlooked. Results from this study show that wind erosion in the JER could alter the spatial heterogeneity of SOC and other soil nutrients significantly over 2–3 years, despite the plant community differences between the two study sites. The overall results of enhanced wind on the grass cover reduction plots are threefold (1) the depletion and redistribution of soil analytes, including significant nutrient loss and decline in overall spatial variation; (2) the disappearance of small, strong fertile islands associated with grasses, implied by the decrease of the magnitude of spatial dependence of SOC and other soil nutrients; and finally (3) the reinforcement of large fertile islands associated with mesquite shrubs, which is indicated by the increase of the range of spatial autocorrelation. We suggest that the change of SOC and soil nutrient spatial patterns induced by enhanced wind erosion may persist and reinforce soil islands associated with shrubs, thus allowing a positive feedback for further desertification in this arid grassland.

Acknowledgements This research was supported by the National Science Foundation (Grant DEB-0316320) and Jornada Basin LTER project (Grant DEB-0080412). We thank Jacquie Hui, Mike Abrams, Emilee Carpenter, Melissa Castiano, and Tom Zhao for their assistance in experimental set up, sample collection, and laboratory analysis. Special appreciation is given to the headquarters of the USDA-ARS JER staff Kris Havstad, Eddie Garcia, Rob Dunlap, David Thatcher and John Anderson, who provided invaluable assistance with field work during this study. Associate editor Dr. Holm Tiessen and two anonymous reviewers made valuable comments that significantly improved the strength and clarity of this paper.

Appendix

Summary of the semivariogram model parameters for wind erosion enhanced (T100) and control plots in 2004 and 2005. All parameters were described in the Table 4 legend

Analyte	A_0 (m)		$C/(C_0 + C)$		MSR	
	T100	Control	T100	Control	T100	Control
(a) *Sporobolus*-mesquite site						
July 2004						
SOC	1.89 (0.35)*	1.01 (0.78)	0.78 (0.07)	0.52 (0.18)	0.04	−0.09
TN	1.54 (0.24)	1.63 (0.39)	0.78 (0.11)	0.51 (0.54)	0.09	−0.06
N_{avail}	2.22 (0.35)*	0.65 (0.27)	0.69 (0.10)	0.75 (0.20)	0.04	−0.15
PO_4^{3-}	>3.0*	1.65 (0.59)	0.83 (0.12)	0.56 (0.15)	0.03	−0.03
K^+	<0.2	1.57 (0.43)	–	0.62 (0.18)	0.11	0.03
Mg^{2+}	0.65 (0.18)*	1.41 (0.26)	0.95 (0.21)*	0.58 (0.10)	0.15	0.04
Ca^{2+}	0.70 (0.22)	<0.2	0.99 (0.20)	–	0.16	0.03
SO_4^{2-}	2.44 (0.37)	1.83 (0.28)	0.81 (0.16)	0.93 (0.16)	−0.11	−0.11
Cl^-	1.88 (0.31)*	>3.0 (0.39)	0.90 (0.14)	0.89 (0.08)	0.07	0.12
Na^+	<0.2	<0.2	–	–	–	–
July 2005						
SOC	>5.0*	0.46 (0.17)	1.00 (0.09)	0.74 (0.29)	0.09	0.13
TN	3.65 (0.51)*	0.49 (0.17)	0.71 (0.13)	0.99 (0.24)	0.04	0.14
N_{avail}	2.25 (0.29)	<0.2	0.99 (0.09)	–	0.0	–
PO_4^{3-}	1.45 (0.24)	1.81 (0.25)	0.91 (0.14)	0.82 (0.11)	0.06	0.02
K^+	1.34 (0.23)	<0.2	0.99 (0.13)	–	0.07	–
Mg^{2+}	1.26 (0.23)	1.27 (0.36)	0.99 (0.15)	0.67 (0.24)	0.15	0.0
Ca^{2+}	1.35 (0.22)	1.51 (0.23)	0.99 (0.12)	0.99 (0.08)	0.04	0.1
SO_4^{2-}	0.78 (0.25)	<0.2	0.99 (0.23)	–	0.05	–
Cl	1.31 (0.30)	<0.2	0.99 (0.18)	–	0.07	–
Na^+	1.20 (0.27)	<0.2	0.94 (0.16)	–	0.10	–
(b) *Bouteloua*-mesquite site						
July 05						
SOC	3.68 (0.38)*	0.57 (0.18)	0.74 (0.10)	0.99 (0.20)	0.04	0.04
TN	1.04 (0.31)	0.77 (0.28)	0.73 (0.20)	0.88 (0.32)	0.04	0.03
N_{avail}	1.63 (0.27)	1.28 (0.23)	0.87 (0.14)	0.85 (0.34)	−0.09	0.07
PO_4^{3-}	1.93 (0.23)*	1.17 (0.22)	0.99 (0.11)	0.86 (0.33)	0.08	0.08
K^+	0.90 (0.19)	–	0.99 (0.18)	–	0.1	–
Mg^{2+}	0.70 (0.32)	0.43 (0.18)	0.60 (0.22)	0.95 (0.29)	0.07	0.03
Ca^{2+}	0.97 (0.21)	1.07 (0.28)	0.99 (0.16)	0.78 (0.42)	0.01	0.13
SO_4^{2-}	0.64 (0.44)	–	0.95 (0.37)	–	−0.05	0.16

Appendix continued

Analyte	A_0 (m)		$C/(C_0 + C)$		MSR	
	T100	Control	T100	Control	T100	Control
Cl^-	0.76 (0.23)	0.75 (0.12)	0.99 (0.17)	0.99 (0.16)	−0.06	0.05
Na^+	2.59 (0.32)	0.63 (0.28)	0.73 (0.14)	0.78 (0.46)	0.12	0.10

References

Augustine DJ, Frank DA (2001) Effects of migratory grazers on spatial heterogeneity of soil nitrogen properties in a grassland ecosystem. Ecology 82:3149–3162

Baldock JA, Nelson PN (2000) Soil organic matter. In: Sumner ME (ed) Handbook of soil science. CRC Press, Boca Raton, FL, pp B25–B84

Buffington LC, Herbel CH (1965) Vegetation changes on a semidesert grassland range from 1858–1964. Ecol Monogr 35:139–164

Bulloch HE Jr, Neher RE (1977) Soil survey of Dona County area, New Mexico. Soil Conserv. Serv., U. S. Dep. of Agric., Washington, DC

Burke IC (1989) Control of nitrogen mineralization in a sagebrush steppe landscape. Ecology 70:1115–1126

Cain ML, Subler S, Evans JP, Fortin MJ (1999) Sampling spatial and temporal variation in soil nitrogen availability. Oecologia 118:397–404

Coppinger KD, Reiners WA, Burke IC, Olson RK (1991) Net erosion on a sagebrush steppe landscape as determined by cesium-137 distribution. Soil Sci Soc Am J 55:254–258

Crawford CS, Gosz JR (1982) Desert ecosystems: their resources in space and time. Environ Conserv 9:181–195

Cross AC, Schlesinger WH (2001) Biological and geochemical controls on phosphorus fractions in semiarid soils. Biogeochemistry 52:155–172

Fisk MC, Schmidt SK, Seastedt TR (1998) Topographic patterns of above- and belowground production and nitrogen cycling in alpine tundra. Ecology 79:2253–2266

Franzluebbers AJ, Stuedemann JA, Schomberg HH (2000) Spatial pattern of soil carbon and nitrogen pools under grazed tall fescue. Soil Sci Soc Am J 64:635–639

Fryrear DW (1986) A field dust sampler. J Soil Water Conserv 41:117–120

Gillette DA, Pitchford AM (2004) Sand flux in the northern Chichuhuan desert, New Mexico, USA, and the influence of mesquite-dominated landscapes. J Geophys Res 109:F04003

Gillette DA, Fryrear DW, Gill TE, Ley T, Cahill TA, Gearhart EA (1997) Relation of vertical flux of particles smaller than 10 μm to aeolian horizontal mass flux at Owens Lake. J Geophys Res 102:26,009–26,015

Gillman GP, Bruce RC, Davey BG, Kimble JM, Searle PL, Skjemstad JO (1983) A comparison of methods used for determination of cation exchange capacity. Commun Soil Sci Plant Anal 14:1005–1014

Goovaerts P (1997) Gostatistics for natural resources evaluation. Oxford University Press, New York, USA

Hartley AE, Barger N, Belnap J et al (2007) Dryland ecosystems. In: Marschner P, Rengel Z (eds) Nutrient cycling in terrestrial ecosystems. Springer

Helm P, Breed CS (1999) Monitoring surface changes in desert areas. In: Breed CS, Reheis MC (eds) Desert winds: monitoring wind-related surface processes in Arizona, Mexico and California. US Geological Survey Professional Paper 1598. G.P.O., Washington, USA, pp 30–51

Hendershot WH, Duquette M (1986) A simple barium chloride method for determining cation exchange and exchangeable cations. Soil Sci Soc Am J 50:605–608

Herman RP, Provencio KR, Herrera-Matos J, Toreez RJ (1995) Resource islands predict the distribution of heterotrophic bacteria in Chihuahuan Desert soils. Appl Environ Microbiol 61:1816–1821

Hook PB, Burke IC, Lanenroth WR (1991) Heterogeneity in soil N and C associated with individual plants and openings in North American shortgrass steppe. Plant Soil 138(2):247–256

Horn OP, Alley MM, Bertsh PM (1982) Cation exchange capacity measurements. Commun Soil Sci Plant Anal 13:851–862

Huisman JA, Snepvangers JJJC, Bouten W, Heuvelink GBM (2003) Monitoring temporal development of spatial soil water content variation: comparison of ground penetrating radar and time domain reflectometry. Vadose Zone 2: 519–529

Isaaks EH, Srivastava RM (1989) An introduction to applied geostatistics. Oxford University Press, New York

Jackson RB, Caldwell MM (1993) Geostatistical patterns of soil heterogeneity around individual perennial plants. J Ecol 81:683–692

Kieft TL, White CS, Loftin SR, Aguilar R, Craig JA, Skaar DA (1998) Temporal dynamics in soil carbon and nitrogen resources at a grassland-shrubland ecotone. Ecology 79(2):671–683

Lajtha K, Schlesinger WH (1988) The biogeochemistry of phosphorus cycling and phosphorus availability along a desert soil chronosequence. Ecology 69(1):24–39

Larney FJ, Bullock MS, Janzen HH, Ellert BH, Olson ES (1998) Wind erosion effects on nutrient redistribution and soil productivity. J Soil Water Conserv 53(2):133–140

Leys J, McTainsh G (1994) Soil loss and nutrient decline by wind erosion-cause for concern. Aust J Soil Water Conserv 7(3):30–40

Li J, Okin GS, Alvarez L, Epstein H (2007) Quantitative effects of vegetation cover on wind erosion and soil nutrient loss in a desert grassland of southern New Mexico, USA. Biogeochemistry 85:317–332

Ludwig JA, Reynolds JF, Whitson PD (1975) Size-biomass relationships of several Chihuahuan Desert shrubs. Am Midl Nat 94:451–461

Nash MS, Jackson E, Whitford WG (2004) Effects of intense, short-duration grazing on microtopography in a Chihuahuan Desert grassland. J Arid Environ 56:383–393

Okin GS, Gillette DA (2001) Distribution of vegetation in wind-dominated landscapes: implications for wind erosion modeling and landscape processes. J Geophys Res 106:9673–9683

Pardo-Iguzquiza E, Dowd P (2001) Variance-covariance matrix of the experimental variogram: assessing variogram uncertainty. Math Geol 33(4):397–419

Parsons AJ, Abrahams AD, Simanton JR (1992) Microtopography and soil-surface materials on seim-arid piedmont hillslopes, southern Arizona. J Arid Environ 22:107–115

Press WH, Teukolsky SA, Vetterling WT, Flannery BP (1992) Numerical recipes in C: the art of scientific computing, 2nd edn. Cambridge University Press, Cambridge, 944 pp

Reynolds JF, Virginia RA, Kemp RR, de Soyza AG, Tremmel DC (1999) Impact of drought on desert shrubs: effects of seasonality and degree of resource island development. Ecol Monogr 68:69–106

Schade JD, Hobbie S (2005) Spatial and temporal variation in islands of fertility in the Sonoran Desert. Biogeochemistry 73:541–553

Schlesinger WH, Pilmanis AM (1998) Plant-soil interactions in deserts. Biogeochemistry 42:169–187

Schlesinger WH, Reynolds J, Cunningham G, Huenneke L, Jarrell W, Virginia R, Whitford W (1990) Biological feedbacks in global desertification. Science 247:1043–1048

Schlesinger WH, Raikes AF, Hartley AE, Cross AF (1996) On the spatial pattern of soil nutrients in desert ecosystems. Ecology 77:364–374

Schlesinger WH, Ward TJ, Anderson J (2000) Nutrient losses in runoff from grassland and shrubland habitats in southern New Mexico: II. Field plots. Biogeochemistry 49:69–86

Scholes RJ, Walker BH (2004) An African savanna-synthesis of nylsvley study. Cambridge University Press, Cambridge, UK

Shafer JM, Varljen MD (1990) Approximation of confidence-limits on sample semivariograms from single realizations of spatially correlated random-fields. Water Resour Res 26(8):1787–1802

Stelzenmüller V, Ehrich S, Zauke GP (2006) Analysis of meso scaled spatial distribution of dab *Limanda limanda* in the German Bight: does the type of fishing gear matter? Fish Sci 72:95–104

Tongway DJ, Hindley N (2000) Assessing and monitoring desertification with soil indicators. In: Arnalds O, Archer S (eds) Rangeland desertification. Kluwer Academic Publishers, Dordrecht, pp 89–98

Troeh FR, Thompson LM (2005) Soil and soil fertility. Blackwell Publishing, Ames, IA, USA

Virginia RA, Jarrell WM (1983) Soil properties in a mesquite-dominated Sonoran Desert ecosystem. Soil Sci Soc Am J 47:138–144

Wang L, Mou PP, Huang J, Wang J (2007) Spatial heterogeneity of soil nitrogen in a subtropical forest in China. Plant Soil 296:137–150

Webster R, Oliver MA (2000) Geostatistics for environmental scientists. Wiley, UK

West NE, Skujins J (1977) The nitrogen cycle in North American cold-winter semi-desert ecosystems. Oecol Plant 12:45–53

Whitford W (2002) Ecology of desert systems. Academic Press, London, UK